



A General Scaling Law of Vascular Tree: Optimal Principle of Bifurcations in Pulsatile Flow

M. Shumal, M. Saghafian[†], E. Shirani, and M. Nili-Ahmadabadi

Department of Mechanical Engineering, Isfahan University of Technology, Isfahan, Iran

[†]Corresponding Author Email: saghafian@iut.ac.ir

ABSTRACT

Murray's law, as the best-known optimal relationship between bifurcation calibers, is obtained based on the assumption of steady-state Poiseuille blood flow and is mostly accurate in small vessels. In middle sized and large vessels such as the aorta and coronary arteries, the pulsatile nature of the flow is dominant and deviations from Murray law have been observed. In the present study, a general scaling law is proposed, which describes the optimum relationship between the characteristics of bifurcations and pulsatile flow. This scaling law takes into account the deviations from Murray law in large vessels, and proposes optimal flow (i.e. less flow resistance) for the full range of the vascular system, from the small vessels to large ones such aorta. As a general scaling law, it covers both symmetrical and asymmetrical bifurcations. One of the merits of this scaling law is that bifurcation characteristics solely depend on the Womersley number of parent vessels. The diameter ratios suggested by this scaling law are in acceptable agreement with available clinical morphometric data such as those reported for coronary arteries and aortoiliac bifurcations. A numerical simulation of pulsatile flow for several Womersley numbers in bifurcation models according to the proposed scaling law and Murray law has been performed, which suggests that the general scaling law provides less flow resistance and more efficiency than Murray law in pulsatile flow.

Article History

Received October 10, 2023

Revised February 28, 2024

Accepted April 17, 2024

Available online July 31, 2024

Keywords:

Pulsatile flow

Womersley number

Murray law

Vascular tree

Scaling law

Flow resistance

1. INTRODUCTION

Arterial bifurcations are prone to atherosclerosis due to abnormal hemodynamics (Asakura & Karino, 1990; Kimura et al., 1996; Morbiducci et al., 2016; Murasato et al., 2022). Considering the risk of restenosis, interventional treatment of these lesions is also a major concern (Tanabe et al., 2004; Lefèvre et al., 2005; Arquizan et al., 2011; Lammeren et al., 2011; Müller et al., 2019; Elsayed et al., 2021). Therefore, it gets higher priority to avoid abnormal hemodynamics. The bifurcation angle and diameter ratio effectively determine the hemodynamic parameters at bifurcations (Huo et al., 2012). The principle of optimal design states that biological structures are optimally selected in nature and should be maintained to avoid any abnormal variation in hemodynamic stresses (Rossitti & Löfgren, 1993). Murray was one of the first who established a relation for the optimal branching pattern of a vascular system based on the steady-state Poiseuille blood flow assumption (Murray, 1926b). Murray's law also known as cubic law expresses that minimum energy is achieved when

volumetric flow is directly related to the third power of vessel radius. This relation is derived from a cost function, using the calculus of variations. The cost function comprises frictional and metabolic energies. These two terms should be compromised since their relation to the radius of the vessel is opposite. Murray's law might be regarded as pumping power with the volume constraint which results in a cubed diameter expression as $D_0^3 = D_1^3 + D_2^3$. The exponent in Murray's law is supported for all trees whose internal flows obey steady-state Poiseuille blood flow assumption such as small arteries, arterioles, and bronchial trees of lungs (Horsfield & Cumming, 1967; Zamir et al., 1983; Kassab & Fung, 1995; Kaimovitz et al., 2008). However, deviations have been observed and different exponents have been reported in bifurcations of the aorta, the pulmonary trunk, coronary arteries, common carotid artery, and major arteries within the Circle of Willis (Sherman, 1981; Ingebrigtsen et al., 2004; Finet et al., 2008; Beare et al., 2011; Huo et al., 2012; Baharoglu et al., 2014). Several studies have been carried out to determine the optimum exponent by assuming different constraints for the cost function which

NOMENCLATURE			
ϑ	kinematic viscosity	l	length of vessel
μ	dynamic viscosity	n	natural number, optimal exponent of diameter ratio
ρ	density	N	Fourier series modes
λ	Lagrange multiplier	p	pressure
φ	aggregate function	Q	blood flow rate
β	daughter to mother diameter ratio	r	radius direction
α	complex form of Womersley number	R	vessel radius
γ	daughter to mother diameter ratio	Res	flow resistance
θ	half of bifurcation angle	t	time
ω	angular frequency of the oscillation	u	the axial component of velocity
A	amplitude of oscillation	Wo	dimensionless Womersley number
D	vessel diameter	x	dummy variable, length direction

usually ranges between 2 and 3 (Mayrovitz, 1987; Uylings, 1977; Dawson et al., 1999; Cebral et al., 2003; Huo & Kassab, 2009). Most of these studies focused on steady-state Poiseuille blood flow assumption, while, typically in large vessels, which deviate from Murray’s law, the pulsatile nature of flow is dominant.

A fundamental functional parameter of a vascular system is the hydraulic resistance, which determines the transport efficiency. Efficiency means maintaining the continuity of flow at a low energy cost, minimizing the specific constraint of the system, and simultaneously avoiding abnormal hemodynamics. In the present study, we propose an optimum relation between the characteristics of parent and branch vessels based on the minimization of the hydraulic resistance to a pulsatile flow. What we believe is a novel scaling law, extends beyond the arterial trees and covers the full range of vascular system from aorta to capillaries. The major significance of the present study is that bifurcation characteristics are solely related to the Womersley number of parent vessels. Unlike most previous studies, the corresponding exponent of the optimality relationship is determined according to the location and diameter of the parent vessel. The scaling law is provided in the symmetrical and asymmetrical bifurcations. The scaling law is validated through numerical simulation of flow for several Womersley numbers in bifurcations modeled according to the proposed scaling law and Murray law diameter ratios and their respective angle rules. It is illustrated that flow resistance in the proposed scaling law bifurcations is less than that of Murray.

2. MATERIAL AND METHOD

2.1 Analytical Method

The governing equation for blood flow in large arteries is the Navier-Stokes equation for laminar incompressible Newtonian fluid, which is simplified and expressed as Eq. (1). Womersley solved this equation and stated the velocity profile as prescribed in Eq. (2) (Womersley, 1955), regarding an oscillating pressure gradient like as $Ae^{i\omega t}$.

$$\frac{1}{\nu} \frac{\partial u}{\partial t} = -\frac{1}{\nu} \frac{\partial p}{\partial x} + \frac{\partial^2 u}{\partial r^2} + \frac{1}{r} \frac{\partial u}{\partial r} \quad (1)$$

$$u(r, t) = \text{Re} \left\{ \frac{A}{i\omega\rho} e^{i\omega t} \left(1 - \frac{J_0(i^{3/2} \sqrt{\frac{\omega}{\nu}} r)}{J_0(i^{3/2} \sqrt{\frac{\omega}{\nu}} R)} \right) \right\} \quad (2)$$

The blood flow rate can be obtained according to Eq. (3) by integrating the velocity profile on the tube’s cross-section (Painter et al., 2006). Where ρ is the fluid density, R is vessel radius, and J_0 and J_2 are the Bessel functions of order 0 and 2, respectively. Regarding ϑ as kinematic viscosity and ω as the angular frequency of the oscillation, the Womersley number, Wo , is a dimensionless number that relates pulsatile flow frequency to viscous effects and is defined as $\sqrt{\frac{\omega}{\nu}} R$.

$$Q_{osc}(t) = -\frac{\pi AR^2}{i\omega\rho} e^{i\omega t} \frac{J_2(\alpha)}{J_0(\alpha)} \quad (3)$$

$$\alpha = i^{3/2} \cdot Wo$$

Based on this equation, the hydraulic resistance to pulsatile flow for a cylindrical tube, as the ratio of overall pressure drop to the total flow rate, can be derived through Eq. (4).

$$Res_{osc} = \frac{\Delta P}{Q} = -i \frac{\omega\rho}{\pi} \frac{l}{R^2} \left[\frac{J_0(\alpha)}{J_2(\alpha)} \right] \quad (4)$$

In human arteries under normal physiological conditions, the pressure cycles from systolic to diastolic values, resulting in a forward pumping pressure gradient, and oscillating pressure gradients. Consequently, the blood flow rate is a periodic function of time. With sufficient regularity, and also regarding the superposition principle, the blood flow rate can be treated as steady and oscillating parts approximated by N complex Fourier modes given in the form of Eq. (5).

$$Q(t) = \sum_{n=0}^N Q_n e^{i\omega n t} = Q_s + \sum Q_{osc} \quad (5)$$

The relationship between flow rate and pressure drop in a fully developed laminar regime is expressed in Eq. (6) (Razavi et al., 2014). For a symmetrical bifurcation illustrated in Fig. 1, the global flow resistance was obtained as Eq. (7), which is an aggregate of steady and oscillating parts (see Appendix).

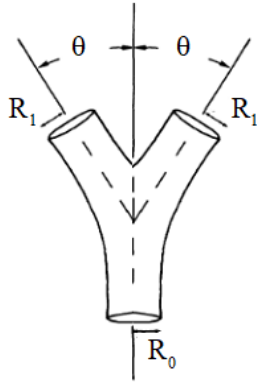


Fig. 1 Schematic of a symmetrical bifurcation

According to constructal theory (Bejan & Lorente, 2008), optimum flow structure is obtained through minimizing the flow resistance. Therefore, Res_i was analytically minimized subjecting to a constant volume constraint, by the use of the method of Lagrange multipliers, which is equivalent to seeking the extremum of the aggregate function of ϕ in Eq. (8). This way, the diameter ratio between daughter and mother in a bifurcation is achieved.

$$\Delta p_s = \left(\frac{8\mu l}{\pi R^4} \right) Q_s \quad (6)$$

$$Res_i = \frac{8\mu}{\pi} \left[\frac{l_0}{R_0^4} + \frac{l_1}{2R_1^4} \right] +$$

$$\frac{\omega\rho}{i\pi} \left[\frac{l_0}{R_0^2} \sum_{n=1}^N n \frac{J_0(\alpha_n)}{J_2(\alpha_n)} + \frac{l_1}{2R_1^2} \sum_{n=1}^N n \frac{J_0(\beta\alpha_n)}{J_2(\beta\alpha_n)} \right] \quad (7)$$

$$\alpha_n = i^{3/2} \sqrt{n} Wo$$

$$\phi = Res_i + \lambda\pi(l_0R_0^2 + 2l_1R_1^2) \quad (8)$$

2.2 Numerical Method

The proposed scaling law (pulsatile optimality rules) is validated using CFD tools. Flow patterns in artery bifurcations constructed according to pulsatile scaling and Murray law are numerically simulated and compared. Ideal Y-shape bifurcations are generated with smooth tubes. The dimensions would be designated by equating a constant volume in both geometries according to Murray and pulsatile rules. The Navier-Stokes and continuity equations are solved through a viscous 3D code employing the finite volume method. Spatial coupling of equations is maintained, utilizing second-order upwind and second-order backward Euler schemes for spatial and time discretization, respectively. Results are acquired at each time step, ensuring all RMS residuals are less than 10^{-5} , and computations are extended over three cardiac cycles. A structured mesh comprising approximately 500,000 hexahedral elements is implemented. Mesh dependency analysis is conducted to achieve a relative error of less than 1% for blood flow rate and time-averaged flow resistance. The total number of time steps per cardiac cycle remains constant at 500 for all cases, utilizing a

uniform time step. Blood density and viscosity are set to 1056 kg/m³ and 3.5 cP, respectively. Blood flow is considered Newtonian, which is an acceptable assumption for large arteries (Vlachopoulos et al., 2011; Haghghi et al., 2016). All tube walls are considered rigid with a no-slip condition. At the inlet boundary, the velocity is set to a Womersley profile as Eq. 2, and on outflow boundaries, the average pressure is set to a constant reference value of 100 mmHg (Alnæs et al., 2007; Harris et al., 2023). Initially, a steady-state Poiseuille flow condition with a parabolic axial velocity profile is assumed (Haghghi et al., 2015). The flow resistance obtained in the last cycle is then compared for each geometry.

3. RESULTS

3.1 Analytical Results

Derivative of Eq. (8) with respect to the radius gives a system of equations for mother and daughter diameters as a function of Lagrange multiplier (λ) which is presented in the Appendix. Solving the system of equations and eliminating λ yields the diameter ratio for a symmetrical bifurcation demonstrated by β in Eq. (9). This equation proposes that in pulsatile flow, β as the caliber of a symmetrical bifurcation, depends on Wo number of mother branch and thus changes based on vessel size from the aorta to fine capillaries. This equation can be shown as Eq. (10), which is more generalized since is expressed in the form of optimal exponent (n). For steady-state Poiseuille flow, as reported by Murray n is equal to 3 (Murray, 1926b).

$$\beta = \frac{D_1}{D_0} = \text{Re} \left\{ \frac{\left[32 - i\beta^3 Wo^2 R_0 \sum_{n=1}^N n f(\beta\alpha_n) \right]^{1/6}}{\left[128 - 4i Wo^2 R_0 \sum_{n=1}^N n f(\alpha_n) \right]} \right\} \quad (9)$$

$$f(\alpha) = \frac{J_1(\alpha)}{J_2^2(\alpha)} [J_0(\alpha) + J_2(\alpha)]$$

$$\frac{D_1}{D_0} = 2^{-1/n} \quad (10)$$

Following the method suggested by Rosen (Rosen, 2013) for a pulsatile flow condition, the angle between daughters (2θ) as another characteristic of the bifurcation is computed by Eq. (11). Where R_0 is the radius of the mother branch (see Appendix).

$$\cos(\theta) = \frac{1}{2} \text{Re} \left\{ \frac{h(1, R_0) + R_0^2}{h(\beta, \beta R_0) + (\beta R_0)^2} \right\} \quad (11)$$

$$h(x, r) = \frac{8 - ix^2 Wo^2 \sum_{n=1}^N n \frac{J_0(x\alpha_n)}{J_2(x\alpha_n)}}{r^2 - \frac{ix^2 Wo^2}{2r} \sum_{n=1}^N n f(x\alpha_n)}$$

β and θ are the main characteristics of a symmetrical bifurcation. All the optimal relations proposed for bifurcation in pulsatile flow from Eqs. 9 to 11 are

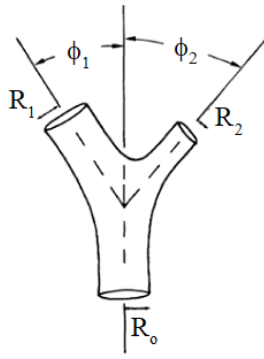


Fig. 2 Schematic of an asymmetrical bifurcation

dependent on Wo of the mother branch, which means suggested optimum values vary depending on vessel size and optimum values for arteries differ from capillaries. Besides that, if Wo tends to zero, equivalent to flow condition in capillaries, β and θ lead to 0.7937 and 37.5° respectively which are similar values reported by Murray (Murray, 1926a).

For asymmetrical bifurcations, similar to Fig. 2, considering only the oscillating part of the flow rate as Eq. (3), the flow resistance in pulsatile flow is calculated based on Eq. (12). This is the analog of impedance matching at the junctions of electrical transmission lines. β and γ are the two diameter ratios of daughters to mother branch. This equation might be simplified as Eq. (13), where n as the exponent, changes based on Wo and is obtained from Eq. (12).

$$\text{Re} \left\{ \frac{f(i^{3/2} \gamma Wo)}{f(i^{3/2} \beta Wo)} \beta^3 + \gamma^3 + 2(\gamma \beta)^{3/2} \left(\frac{f(i^{3/2} \gamma Wo)}{f(i^{3/2} \beta Wo)} \right)^{1/2} = \frac{f(i^{3/2} \gamma Wo)}{f(i^{3/2} Wo)} \right\} \quad (12)$$

$$\beta^n + \gamma^n = 1 \quad (13)$$

Considering Womersley velocity inlet as Eq. (2), Eq. (10) and Eq. (13), the optimal exponent of diameter ratio (n) for symmetrical and asymmetrical bifurcations is illustrated in Fig. 3. This figure shows that (n) ranges based on Wo from 3 in small arterioles and capillaries (where Wo tends to 0) to about 2 in larger vessels such as aortoiliac bifurcation. The trend is the same for both symmetrical and asymmetrical bifurcations and comprises three distinct zones. In the first zone, which includes capillaries, arterioles, and small arteries, Wo is less than 2 and the exponent is equal in both types of bifurcations. Also, in the fully pulsatile zone ($Wo > 7$), symmetrical and asymmetrical bifurcations report close values for optimal exponent with less than 1% difference. The main distinction between symmetrical and asymmetrical bifurcations is observed for middle-sized vessels such as cerebral arteries and coronary arteries with Wo between 2 to 5. This zone is called the transitional zone from quasi-steady to fully pulsatile flow. The maximum difference in this zone is also small and is below 6%. Therefore, for the artery flows with a forward pumping pressure gradient

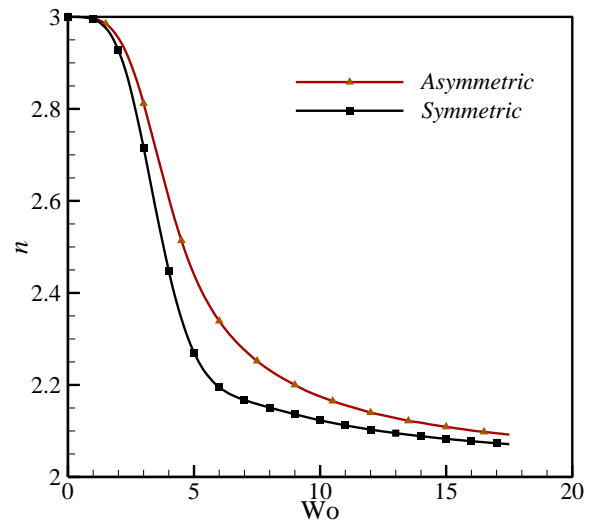


Fig. 3 Optimal diameter ratio for bifurcations as a function of Wo

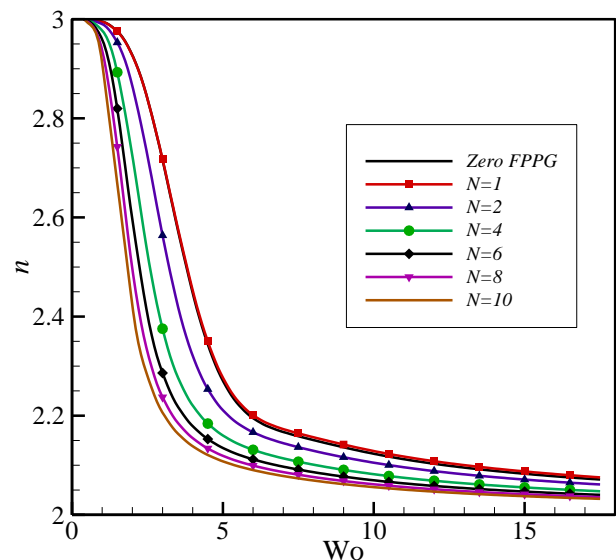


Fig. 4 Exponent of optimal diameter ratio equation as a function of Wo for different Fourier modes in a symmetrical bifurcation

(FPPG), the equivalent exponent predicted by Eq. (9) might be implemented in Eq. (13) to find the optimum relationship between branches' diameter ratios in asymmetrical bifurcations.

Equation. (9) and Eq. (11) express that optimum calibers depend on Wo and the number of Fourier modes. Fig. 4 illustrates the trend of the exponent of optimal diameter ratio (n) for different Fourier modes. It is evident that the presence of FPPG does not affect the overall tendency of the optimal diameter ratio, and the line of harmonic oscillatory flow with a positive pumping pressure gradient ($N=1$) mimics the zero FPPG flow, Eq. (3). Increasing the number of harmonic modes reduces the value of the optimal exponent, indicating that transient inertial forces dominate and quasi-steady flow zone shrinks.

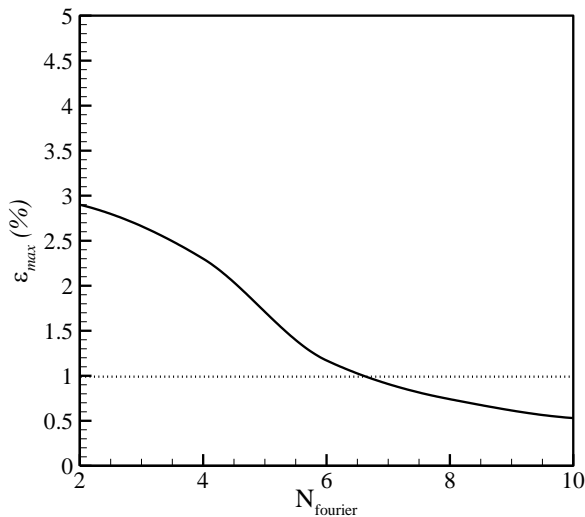


Fig. 5 The maximum difference of exponent values according to changes in the order of the Fourier series

The values obtained by the line of eight Fourier modes ($N=8$) might be considered target values since most of the blood flow rate profiles can be approximated using the Fourier series with eight modes. Moreover, as shown in Fig. 5, the maximum difference between the reported n values by $N=6$ and $N=8$ lines is less than 1%.

Figure. 6 shows the angle of symmetrical bifurcation for zero FPPG inflow and positive FPPG inflow with eight Fourier modes. This figure indicates that larger vessels with larger Wo bifurcate at smaller angles. By increasing the branching generation, the vessel diameter and as a consequence, Wo decreases. Thus, the angle of bifurcations increases and in arterioles and capillaries reaches the reported value by Murray as 75° . This concept is supported by reported clinical studies. Those three distinct zones are also noticeable for optimal angle distribution over the vessel size range. It is interpreted that FPPG would cause a dump in the influence of viscous forces and shift the values to the fully pulsatile zone.

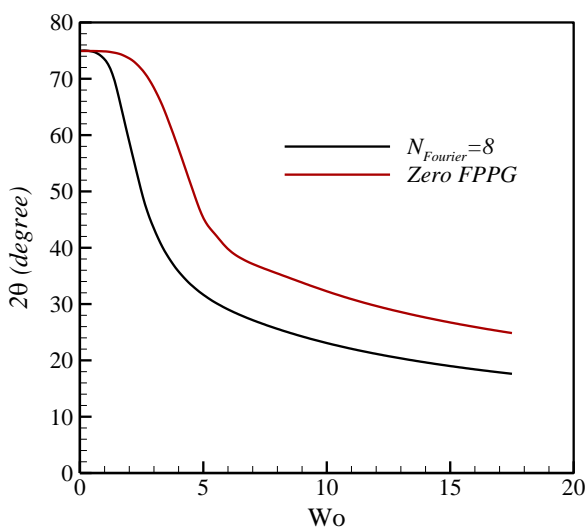


Fig. 6 Optimal bifurcation angle as a function of Wo (considering the number of Fourier modes effect)

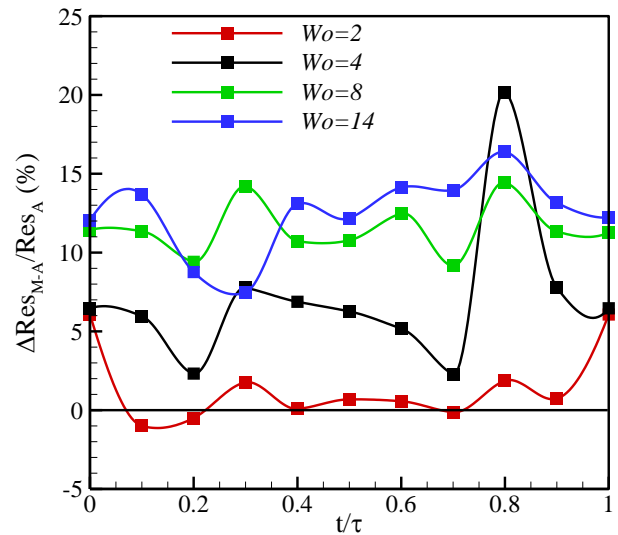


Fig. 7 Flow resistance difference between pulsatile optimality and Murray's law for Womersley numbers (Wo) of 2, 4, 8, and 14

3.2 Numerical Validation

The reported values of optimal calibers obtained from the above equations are validated through numerical simulation. Fig. 7 shows the difference in flow resistance determined by numerical simulation of the bifurcations constructed based on the proposed scaling law and Murray law for four distinct inflow Wo . Positive values indicate higher resistance in Murray law-based geometries and consequently higher energy and cost demand. Due to the almost completely positive yielded resistance difference for all inflow Wo 's, it is obvious that the energy losses are higher in Murray law-based configurations. In quasi-steady flow with $Wo=2$, since the calibers of pulsatile optimality and Murray law are almost the same, flow resistance in Murray's is only about 2% higher. However, even this slight difference makes the pulsatile optimality rules more efficient. As Wo increases, transient inertial forces become more dominant, and deviation from Murray's law is more significant. The time-averaged flow resistance difference between the proposed scaling law and Murray law increases as Wo increases from 4 to 14. For $Wo=14$, the equivalent exponent (n) is 2.09 which is noticeably different from Murray's reported value of $n=3$ which causes a 12% increase in flow resistance for Murray's rule-based bifurcations.

4. DISCUSSION

In the cardiovascular system, the pulsation frequency and blood properties are assumed constant, so the Womersley number is dependent on vessel size. As a consequence, according to the presented scaling law, bifurcation calibers would change based on the variations in vessel size across the vascular system. This is one of the remarkable outcomes of the described pulsatile flow optimality relationships. For large vessels with $Wo > 5$, the pulsatile nature of flow predisposes the bifurcation to almost follow an area-preserving law ($n=2$) for minimizing energy loss. This behavior is attributed to

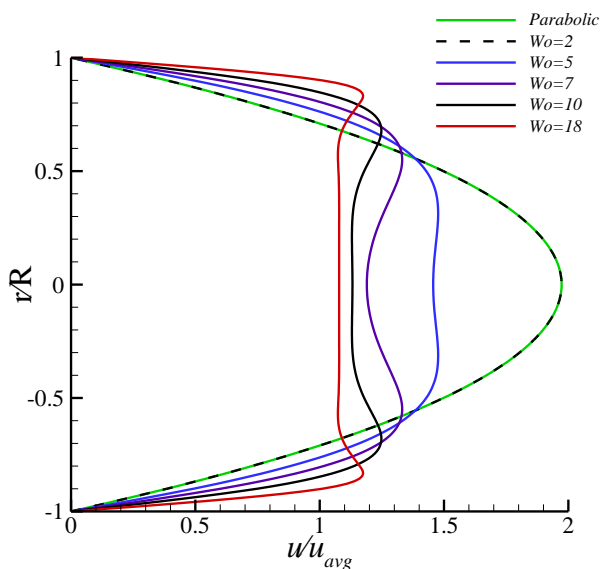


Fig. 8 Scaled velocity profile according to different Womersley numbers (San & Staples, 2012)

changes in the velocity profile, illustrated in Fig. 8, where higher Womersley numbers lead to a plug profile. A plug velocity profile, or constant inflow and outflow velocity at the bifurcation, corresponds to the conservation of the area at the mother and daughter vessels, indicating $n=2$. Thus, the bifurcation angle and diameter ratio are smaller for large vessels.

As the branching generation grows, the vessel size decreases and viscosity forces gradually become more effective. Ultimately, for $Wo < 2$, the viscosity becomes dominant, causing quasi-steady flow with Poiseuille resistance law of $n=3$ as the governing optimal relationship. In these circumstances, the calibers of bifurcation are the same as the values reported by Murray. The uniformity of wall shear stress, independent of vessel diameter, is a direct outcome of Murray's law (Golozar et al., 2017). Figure 9 demonstrates the ratio of time-averaged wall shear stress in mother and daughter vessels for a symmetrical bifurcation in various Womersley numbers. It illustrates the non-linear relationship of wall shear stress to vessel diameter in pulsatile flow. Notably, the ratio approaches unity for $Wo < 2$, affirming the acceptability of the uniform wall shear stress hypothesis in the quasi-steady zone (Painter et al., 2006). At higher Womersley numbers, β decreases, leading to a noteworthy 40% increase in wall shear stress on the daughter vessel. It is important to highlight that the oscillatory components of wall shear stress remain consistent between mother and daughter vessels across different Womersley numbers. In the transitional zone from steady-state to purely oscillatory flow ($2 < Wo < 5$), the transient inertial forces and steady-state Poiseuille resistance are comparable and because of that, a step-like profile is proposed for calibers. Thus, the blood vascular system is constructed in a way that vessels bifurcate according to these relationships. Therefore, while it converts purely oscillatory flow in the aorta to steady-state flow in capillaries, it provides the minimum flow resistance. Considering the human Aorta size, Wo is typically about 14~15. Based on Eq. (9),

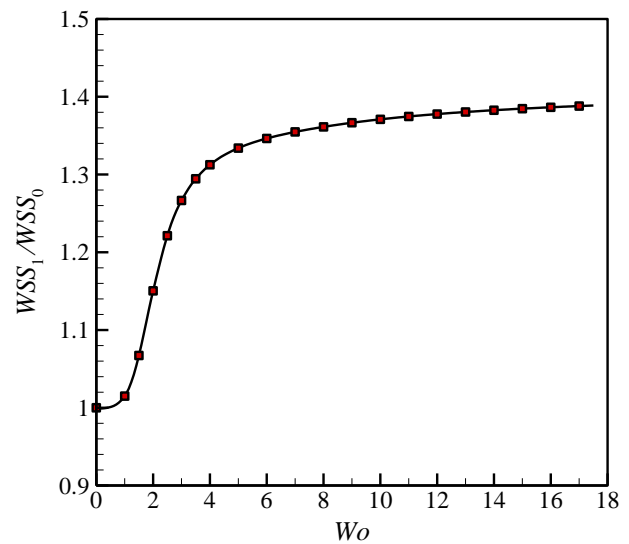


Fig. 9 The ratio of WSS in mother and daughter vessels in symmetrical bifurcation according to different Womersley numbers

steady-state Poiseuille flow initiates just after three branching generations and results in a reduction in Wo to below 5. It would completely dominate the flow after six generations, when Wo decreases to less than 2, exactly as reported by West (West et al., 1997).

Regarding Eq. (9), it needs 34 generations to reach from the Aorta to capillary sizes, which is supported by literature (LaBarbera, 1990). The optimality relationships of pulsatile flow are validated by comparing analytical results with available clinical morphometric data as expressed in Table 1. The Wo was computed based on the reported mother vessel size for each reference, assuming a normal heart beating rate of 70 bpm. With $N=8$ and the computed Wo , analytical values can be proposed using Eq. 9. Table 1 demonstrates that the scaling law has an acceptable agreement with clinical data across each of the three prescribed flow zones. Furthermore, the proposed relationship can explain the significant deviation from Murray law in large arteries, such as the aortoiliac, which is located in the fully pulsatile flow zone. Additionally, for a middle-sized artery such as MCA, which yields optimal values close to Murray law, the exact optimal value is predicted by the proposed scaling law, while others only consider Murray law to be somewhat accepted.

5. CRITIQUE OF MODEL

The compliance of vessels, determined by their elastic properties, plays a crucial role, particularly in large arteries (Quarteroni & Formaggia, 2004). While the assumption of a rigid wall in high Womersley number scenarios may be questioned, studies indicate that the incompressible-fluid, thin-wall approximation for an oscillatory pressure wave applied on an elastic vessel yields consistent results. This approximation, demonstrated in large arteries, shows a step-like behavior with an optimal exponent typically around 2 (West et al., 1997). In small vessels, blood exhibits shear-thinning behavior, necessitating consideration as a non-Newtonian

Table 1 Comparison of the diameter ratio between the proposed analytical equations and experimental studies in coronary arteries, left anterior descending artery (LAD), middle cerebral artery (MCA), and Aortoiliac bifurcations in normal and healthy blood flow conditions

Vessel	W_0	Biological exponent of diameter ratio (Clinical n)		Obtained results for exponent of diameter ratio (Analytical n)
		Data	Ref.	
Coronary Arteries	3.1	2.26	(Finet et al., 2008)	2.22
	2.44	2.35		2.34
	1.63	2.65		2.64
	2	2.66		2.5
LAD	2.66	2.26	(Huo et al., 2012)	2.29
MCA	1.6	2.69	(Baharoglu et al., 2014)	2.69
Aortoiliac	13.9	2.04	(Joh et al., 2013)	2.04
	13.1	1.6		2.04
	12	1.8	(Hu et al., 2022)	2.05
	10.5	1.9		2.06

fluid. However, in large arteries, where deviations from Murray’s law have been documented, blood tends to exhibit Newtonian fluid characteristics (Vlachopoulos et al., 2011; Haghghi et al., 2016). The validity of our proposed results is supported by studies in small arteries (Horsfield & Cumming, 1967; Zamir et al., 1983; Kassab & Fung, 1995; Kaimovitz et al., 2008) and aligns with available morphometric clinical data in large arteries (Finet et al., 2008; Huo et al., 2012; Joh et al., 2013; Baharoglu et al., 2014; Hu et al., 2022). Furthermore, according to (Huo et al., 2012) the wave reflection due to vessel branching (Vosse & Stergiopoulos, 2011) requires a fluid-structure interaction computational model. However, in some cases such as the aorta-carotid interface, a low bifurcation reflection coefficient has been reported (Haidar et al., 2021).

6. CONCLUSION

Murray’s law as the optimum relationship between the characteristics of bifurcations is developed based on the steady-state Poiseuille blood flow assumption and mostly applies to capillaries. Considering the pulsatile flow condition in middle and large sized arteries, we derived and validated a general scaling law, as an extension of Murray’s law to pulsatile flow, which applies to the full range of the vascular tree. It mimics Murray’s law in small vessels, where Womersley number tends to zero. As vessel size increases, the pulsatile nature of the flow becomes dominant, and the bifurcation angle and diameter ratio decrease in a step-like profile.

The proposed scaling law addresses reported deviations from Murray’s law in arteries and is in acceptable agreement with available morphometric vascular data such as those reported for coronary arteries. Numerical simulation of pulsatile flow for several Womersley numbers, suggests that the proposed scaling law provides less flow resistance than Murray law in pulsatile flow.

CONFLICT OF INTEREST

On behalf of all authors, the corresponding author states that there is no competing interest.

AUTHORS CONTRIBUTION

M. Shumal, M. Saghafian, and E. Shirani contributed to developing the main concept of the article. **M. Shumal** developed analytical methods, performed numerical simulation, and wrote the main manuscript text. **M. Saghafian, E. Shirani** and **M. Nili-Ahmadabadi** supervised the findings of the work. All authors reviewed the manuscript carefully.

REFERENCES

- Alnæs, M. S., Isaksen, J., Mardal, K. A., Romner, B., Morgan, M. K., & Ingebrigtsen, T. (2007). Computation of hemodynamics in the circle of willis. *Stroke*, 38(9), 2500-2505. <https://doi.org/10.1161/STROKEAHA.107.482471>
- Arquizan, C., Trinquart, L., Touboul, P. J., Long, A., Feasson, S., Terriat, B., Mettall, M. P. G., Guidolin, B., Cohen, S., & Mas, J. L. (2011). Restenosis Is more frequent after carotid stenting than after endarterectomy. *Stroke*, 42(4), 1015-1020. <https://doi.org/10.1161/STROKEAHA.110.589309>
- Asakura, T., & Karino, T. (1990). Flow patterns and spatial distribution of atherosclerotic lesions in human coronary arteries. *Circulation research*, 66(4), 1045-1066. <https://doi.org/10.1161/01.res.66.4.1045>
- Baharoglu, M. I., Lauric, A., Wu, C., Hippelheuser, J., & Malek, A. M. (2014). Deviation from optimal vascular caliber control at middle cerebral artery bifurcations harboring aneurysms. *Journal of Biomechanics*, 47(13), 3318-3324. <https://doi.org/10.1016/j.jbiomech.2014.08.012>
- Beare, R. J., Das, G., Ren, M., Chong, W., Sinnott, M. D., Hilton, J. E., Srikanth, V., & Phan, T. G. (2011). Does the principle of minimum work apply at the carotid bifurcation: a retrospective cohort study. *BMC Medical Imaging*, 11(1), 1-6. <https://doi.org/10.1186/1471-2342-11-17>

- Bejan, A., & Lorente, S. (2008). *Design with Constructal Theory*. John Wiley & Sons. <https://doi.org/10.1002/9780470432709>
- Cebral, J. R., Castro, M. A., Soto, O., Löhner, R., & Alperin, N. (2003). Blood-flow models of the circle of Willis from magnetic resonance data. *Journal of Engineering Mathematics*, 47(3), 369-386. <https://doi.org/10.1023/b:engi.0000007977.02652.02>
- Dawson, C. A., Krenz, G. S., Karau, K. L., Haworth, S. T., Hanger, C. C., & Linehan, J. H. (1999). Structure-function relationships in the pulmonary arterial tree. *Journal of Applied Physiology*, 86(2), 569-583. <https://doi.org/10.1152/jappl.1999.86.2.569>
- Elsayed, N., Ramakrishnan, G., Naazie, I., Sheth, S., & Malas, M. B. (2021). Outcomes of carotid revascularization in the treatment of restenosis after prior carotid endarterectomy. *Stroke*, 52(10), 3199-3208. <https://doi.org/10.1161/STROKEAHA.120.033667>
- Finet, G., Gilard, M., Perrenot, B., Rioufol, G., Motreff, P., Gavit, L., & Prost, R. (2008). Fractal geometry of arterial coronary bifurcations: a quantitative coronary angiography and intravascular ultrasound analysis. *EuroIntervention*, 3(4), 490-498. <https://doi.org/10.4244/EIJV314A87>
- Golozar, M., Sayed Razavi, M., & Shirani, E. (2017). Theoretical and computational investigation of optimal wall shear stress in bifurcations: a generalization of Murray's law. *Scientia Iranica*, 24(5), 2387-2395. <https://doi.org/10.24200/sci.2017.4506>
- Haghighi, A. R., Asl, M. S., & Kiyasatfar, M. (2015). Mathematical modeling of unsteady blood flow through elastic tapered artery with overlapping stenosis. *Journal of the Brazilian Society of Mechanical Sciences and Engineering*, 37(2), 571-578. <https://doi.org/10.1007/s40430-014-0206-3>
- Haghighi, A. R., Kabdool, A. A., Asl, M. S., & kiyasatfar, M. (2016). Numerical investigation of pulsatile blood flow in stenosed artery. *International Journal of Applied and Computational Mathematics*, 2(4), 649-662. <https://doi.org/10.1007/s40819-015-0084-0>
- Haidar, M. A., van Buchem, M. A., Sigurdsson, S., Gotal, J. D., Gudnason, V., Launer, L. J., & Mitchell, G. F. (2021). Wave reflection at the origin of a first-generation branch artery and target organ protection: The AGES-Reykjavik study. *Hypertension*, 77(4), 1169-1177. <https://doi.org/10.1161/HYPERTENSIONAHA.120.16696>
- Harris, J., Paul, A., & Ghosh, B. (2023). Numerical simulation of blood flow in aortoiliac bifurcation with increasing degree of stenosis. *Journal of Applied Fluid Mechanics*, 16(8), 1601-1614. <https://doi.org/10.47176/JAFM.16.08.1552>
- Horsfield, K., & Cumming, G. (1967). Angles of branching and diameters of branches in the human bronchial tree. *Bulletin of Mathematical Biology*, 29, 245-259. <https://doi.org/10.1007/BF02476898>
- Hu, J., Zheng, Z.-F., Zhou, X. T., Liu, Y. Z., Sun, Z. M., Zhen, Y. S., & Gao, B. L. (2022). Normal diameters of abdominal aorta and common iliac artery in middle-aged and elderly Chinese Han people based on CTA. *Medicine*, 101(31), 1-6. <https://doi.org/10.1097/MD.00000000000030026>
- Huo, Y., & Kassab, G. S. (2009). A scaling law of vascular volume. *Biophysical Journal*, 96(2), 347-353. <https://doi.org/10.1016/j.bpj.2008.09.039>
- Huo, Y., Finet, G., Lefevre, T., Louvard, Y., Moussa, I., & Kassab, G. S. (2012). Which diameter and angle rule provides optimal flow patterns in a coronary bifurcation? *Journal of Biomechanics*, 45(7), 1273-1279. <https://doi.org/10.1016/j.jbiomech.2012.01.033>
- Ingebrigtsen, T., Morgan, M. K., Faulder, K., Ingebrigtsen, L., Sparr, T., & Schirmer, H. (2004). Bifurcation geometry and the presence of cerebral artery aneurysms. *Journal of Neurosurgery*, 101(1), 108-113. <https://doi.org/10.3171/jns.2004.101.1.0108>
- Joh, J. H., Ahn, H. J., & Park, H. C. (2013). Reference diameters of the abdominal aorta and iliac arteries in the Korean population. *Yonsei Medical Journal*, 54(1), 48-54. <https://doi.org/10.3349/ymj.2013.54.1.48>
- Kaimovitz, B., Huo, Y., Lanir, Y., & Kassab, G. S. (2008). Diameter asymmetry of porcine coronary arterial trees: structural and functional implications. *American Journal of Physiology-Heart and Circulatory Physiology*, 294(2), H714-H723. <https://doi.org/10.1152/ajpheart.00818.2007>
- Kassab, G. S., & Fung, Y. C. B. (1995). The pattern of coronary arteriolar bifurcations and the uniform shear hypothesis. *Annals of Biomedical Engineering*, 23, 13-20. <https://doi.org/10.1007/BF02368296>
- Kimura, B. J., Russo, R. J., Bhargava, V., McDaniel, M. B., Peterson, K. L., & DeMaria, A. N. (1996). Atheroma morphology and distribution in proximal left anterior descending coronary artery: in vivo observations. *Journal of the American College of Cardiology*, 27(4), 825-831. [https://doi.org/10.1016/0735-1097\(95\)00551-X](https://doi.org/10.1016/0735-1097(95)00551-X)
- LaBarbera, M. (1990). Principles of design of fluid transport systems in zoology. *Science*, 249(4972), 992-1000. <https://doi.org/10.1126/science.2396104>
- Lammeren, G. W. V., Peeters, W., Vries, J. P. P. M. d., Kleijn, D. P. V. d., Borst, G. J. D., Pasterkamp, G., & Moll, F. L. (2011). Restenosis after carotid surgery. *Stroke*, 42(4), 965-971. <https://doi.org/10.1161/STROKEAHA.110.603746>
- Lefèvre, T., Morice, M. C., Sengottuvel, G., Kokis, A., Monchi, M., Dumas, P., Garot, P., & Louvard, Y. (2005). Influence of technical strategies on the outcome of coronary bifurcation stenting. *EuroIntervention*, 1(1), 31-37. <https://doi.org/10.4244/EIJV111A02>

- Mayrovitz, H. N. (1987). An optimal flow-radius equation for microvessel non-newtonian blood flow. *Microvascular Research*, 34(3), 380-384. [https://doi.org/10.1016/0026-2862\(87\)90069-0](https://doi.org/10.1016/0026-2862(87)90069-0)
- Morbiducci, U., Kok, A. M., Kwak, B. R., Stone, P. H., Steinman, D. A., & Wentzel, J. J. (2016). Atherosclerosis at arterial bifurcations: evidence for the role of haemodynamics and geometry. *Thrombosis and Haemostasis*, 115(03), 484-492. <https://doi.org/10.1160/th15-07-0597>
- Müller, M. D., Gregson, J., McCabe, D. J. H., Nederkoorn, P. J., Worp, H. B. v. d., Borst, G. J. d., Cleveland, T., Wolff, T., Engelter, S. T., Lyner, P. A., Brown, M. M., & Bonati, L. H. (2019). Stent design, restenosis and recurrent stroke after carotid artery stenting in the international carotid stenting study. *Stroke*, 50(11), 3013-3020. <https://doi.org/10.1161/STROKEAHA.118.024076>
- Murasato, Y., Meno, K., Mori, T., & Tanenaka, K. (2022). Impact of coronary bifurcation angle on the pathogenesis of atherosclerosis and clinical outcome of coronary bifurcation intervention—A scoping review. *Plos One*, 17(8), e0273157. <https://doi.org/10.1371/journal.pone.0273157>
- Murray, C. D. (1926a). The physiological principle of minimum work applied to the angle of branching of arteries. *The Journal of General Physiology*, 9(6), 835. <https://doi.org/10.1085%2Fjgp.9.6.835>
- Murray, C. D. (1926b). The physiological principle of minimum work: I. The vascular system and the cost of blood volume. *Proceedings of the National Academy of Sciences*, 12(3), 207-214. <https://doi.org/10.1073/pnas.12.3.207>
- Painter, P. R., Edén, P., & Bengtsson, H. U. (2006). Pulsatile blood flow, shear force, energy dissipation and Murray's Law. *Theoretical Biology and Medical Modelling*, 3(1), 1-10. <https://doi.org/10.1186/1742-4682-3-31>
- Quarteroni, A., & Formaggia, L. (2004). Mathematical modelling and numerical simulation of the cardiovascular system. *Handbook of Numerical Analysis*, 12, 3-127. [https://doi.org/10.1016/S1570-8659\(03\)12001-7](https://doi.org/10.1016/S1570-8659(03)12001-7)
- Razavi, M. S., Shirani, E., & Salimpour, M. (2014). Development of a general method for obtaining the geometry of microfluidic networks. *Aip Advances*, 4(1). <https://doi.org/10.1063/1.4861067>
- Rosen, R. (2013). *Optimality principles in biology*. Springer. <https://doi.org/10.1007/978-1-4899-6419-9>
- Rossitti, S., & Löfgren, J. (1993). Vascular dimensions of the cerebral arteries follow the principle of minimum work. *Stroke*, 24(3), 371-377. <https://doi.org/10.1161/01.STR.24.3.371>
- San, O., & Staples, A. E. (2012). An improved model for reduced-order physiological fluid flows. *Journal of Mechanics in Medicine and Biology*, 12(03), 1250052. <https://doi.org/10.1142/s0219519411004666>
- Sherman, T. F. (1981). On connecting large vessels to small. The meaning of Murray's law. *The Journal of General Physiology*, 78(4), 431-453. <https://doi.org/10.1085/jgp.78.4.431>
- Tanabe, K., Hoye, A., Lemos, P. A., Aoki, J., Arampatzis, C. A., Saia, F., Lee, C. H., Degertekin, M., Hofma, S. H., & Sianos, G. (2004). Restenosis rates following bifurcation stenting with sirolimus-eluting stents for de novo narrowings. *The American journal of cardiology*, 94(1), 115-118. <https://doi.org/10.1016/j.amjcard.2004.03.040>
- Uyilings, H. B. M. (1977). Optimization of diameters and bifurcation angles in lung and vascular tree structures. *Bulletin of Mathematical Biology*, 39(5), 509-520. [https://doi.org/10.1016/S0092-8240\(77\)80054-2](https://doi.org/10.1016/S0092-8240(77)80054-2)
- Vlachopoulos, C., O'Rourke, M., & Nichols, W. W. (2011). *McDonald's blood flow in arteries: theoretical, experimental and clinical principles*. CRC press.
- Vosse, F. N. V. D., & Stergiopulos, N. (2011). Pulse wave propagation in the arterial tree. *Annual Review of Fluid Mechanics*, 43(1), 467-499. <https://doi.org/10.1146/annurev-fluid-122109-160730>
- West, G. B., Brown, J. H., & Enquist, B. J. (1997). A general model for the origin of allometric scaling laws in biology. *Science*, 276(5309), 122-126. <https://doi.org/10.1126/science.276.5309.122>
- Womersley, J. R. (1955). Method for the calculation of velocity, rate of flow and viscous drag in arteries when the pressure gradient is known. *The Journal of Physiology*, 127(3), 553. <https://doi.org/10.1113%2Fjphysiol.1955.sp005276>
- Zamir, M., Wrigley, S., & Langille, B. (1983). Arterial bifurcations in the cardiovascular system of a rat. *The Journal of General Physiology*, 81(3), 325-335. <https://doi.org/10.1085/jgp.81.3.325>

APPENDIX

a. Derivation of Optimal Diameter Ratio in Symmetrical Bifurcation

A symmetric tree structure consists of a parent branch with two identical daughter branches at each level (or generation). The total pressure drop is the sum of pressure drops in the mother and daughter branches. Since the daughter branches are identical, the pressure drops in the mother and daughter branches are the same. Consequently, the total pressure drop (Δp_T) is written as:

$$\Delta p_T = \Delta p_0 + \Delta p_1 \quad (A.1)$$

Where subscripts 0 and 1 denote the mother and daughter branches, respectively. The flow in the mother branch is divided into two daughter branches. Therefore, the total flow rate (Q_T) in the mother branch is twice the flow rate of the daughter branch as follows:

$$Q_T = Q_0 = 2Q_1 \quad (A.2)$$

Using Eqs. (A.1), (A.2), and considering Womersley flow conditions, the global flow resistance of a tree structure is obtained as:

$$Res = -\frac{i\omega\rho}{\pi} \left[\frac{l_0}{R_0^2} \frac{J_0(\alpha_0)}{J_2(\alpha_0)} + \frac{l_1}{2R_1^2} \frac{J_0(\alpha_1)}{J_2(\alpha_1)} \right] \quad (A.3)$$

$$\alpha = i^{3/2}Wo$$

For minimizing Res , an aggregate function of ϕ is obtained by subjecting Res to constant volume constraint as:

$$\phi = Res + \lambda V, \quad V = \pi(l_0 R_0^2 + 2l_1 R_1^2) \quad (A.4)$$

By the use of the method of Lagrange multipliers, and deriving ϕ with respect to R_0 and R_1 the Lagrange multiplier (λ) is computed as follows:

$$\frac{\partial\phi}{\partial R_0} = 0 \rightarrow \frac{\partial Res}{\partial R_0} + \lambda \frac{\partial V}{\partial R_0} = 0, \quad \lambda = \frac{i\omega\rho}{2\pi^2} \cdot \frac{1}{R_0} \left(\frac{J_0(\alpha_0)}{J_2(\alpha_0)} \right)' \quad (A.5)$$

$$\frac{\partial\phi}{\partial R_1} = 0 \rightarrow \frac{\partial Res}{\partial R_1} + \lambda \frac{\partial V}{\partial R_1} = 0,$$

$$\lambda = \frac{i\omega\rho}{8\pi^2} \cdot \frac{1}{R_1} \left(\frac{J_0(\alpha_1)}{J_2(\alpha_1)} \right)'$$

Considering that the required derivative is computed as the following, λ would be obtained.

$$\left(\frac{J_0(\alpha)}{J_2(\alpha)} \right)' = -\frac{\omega}{i.v.\alpha^2} \left(\frac{J_1(\alpha)J_2(\alpha) + J_0(\alpha)J_1(\alpha)}{\alpha^2 J_2^2(\alpha)} \right) \quad (A.6)$$

$$\left(\frac{J_0(\alpha)}{J_2(\alpha)} \right)' = -\frac{J_1(\alpha)}{r^2} \left(\frac{J_2(\alpha) + J_0(\alpha)}{J_2^2(\alpha)} \right)$$

Substituting (A.6) in (A.5), λ can be eliminated from (A.5) by equating those two relations in (A.5). Hence, the diameter ratio is obtained as:

$$\beta = \text{Re} \left\{ 2^{-2/3} \left[\frac{f(\beta i^{3/2} Wo)}{f(i^{3/2} Wo)} \right]^{1/3} \right\} \quad (A.7)$$

$$f(\alpha) = \frac{J_1(\alpha)}{J_2^2(\alpha)} [J_2(\alpha) + J_0(\alpha)]$$

b. Derivation of Optimal Symmetrical Bifurcation Angle

For a single unbranched vessel of length l , the cost function is yielded as:

$$W = Q^2 Res + \Gamma V \quad (B.1)$$

This is differentiated with respect to radius (r) and the result is equated to zero. it is then found that the cost function attains its minimal value when:

$$Q^2 = \frac{2\Gamma\pi^2 i}{\omega\rho} r^3 f^{-1}(\alpha) \quad (B.2)$$

Substituting (B.2) in (B.1), the power dissipation per unit length is related to the radius of the vessel by:

$$\frac{W_{opt}}{l} = \Gamma\pi\psi(r, \alpha) \quad (B.3)$$

$$\psi(r, \alpha) = \left[\frac{2J_0(\alpha)J_2(\alpha)}{J_1(\alpha)} (J_0(\alpha) + J_2(\alpha))^{-1} r + r^2 \right]$$

Where, Γ is a constant and, ψ is a function of radius (for constant flow and fluid properties, α is dependent on radius). If the bifurcation point is displaced by a small displacement δ , the bifurcation angle changes concerning the bifurcation position. Consequently, there are small changes in the lengths and overall cost. For an arbitrarily small displacement (δ), there is an optimum bifurcation position where the variation of overall cost due to small displacement is equal to zero ($\delta W_{opt} = 0$), and for a symmetrical bifurcation results in:

$$\psi(R_0, \alpha_0) \delta l_0 + 2\psi(R_1, \alpha_1) \delta l_1 = 0 \quad (B.4)$$

The optimum bifurcation angle also can be found by taking into account the effect of small displacement δ of the bifurcation point along the mother branch (B.5).

$$\delta l_0 = \delta, \quad \delta l_1 = -\delta \cos(\theta) \quad (B.5)$$

Substituting the (B.5) in (B.4), the optimum bifurcation angle (2θ) is obtained as:

$$\cos(\theta) = \frac{1}{2\beta} \cdot \text{Re} \left\{ \frac{C(i^{3/2}Wo) + R_0}{C(i^{3/2}\beta.Wo) + \beta.R_0} \right\} \quad (B.6)$$

Where β is the optimum diameter ratio and the (C) function is obtained from the (B.7) equation.

$$C(\alpha) = 2 \cdot \frac{J_0(\alpha)J_2(\alpha)}{J_1(\alpha)} [J_0(\alpha) + J_2(\alpha)]^{-1} \quad (B.7)$$

c. Derivation of Optimal Length Ratio in Symmetrical Bifurcation

Considering (V) is constant, the global resistance is dependent on (l_0) and (l_1), but the two vessel lengths

cannot be varied independently because of the area constraint:

$$A_s = l_0 \cdot l_1 \quad (C.1)$$

For obtaining the length ratio, an aggregate function of (ψ) is developed by subjecting ($V.Res$) to area constraint as:

$$\Psi = V.Res + \lambda.A_s \quad (C.2)$$

By the use of the method of Lagrange multipliers, deriving (ψ) with respect to (l_0) and (l_1) and eliminating the (λ), length ratio ($L = l_1/l_0$) is obtained as:

$$L = \frac{l_1}{l_0} = \text{Re} \left\{ \left[\frac{g(i^{3/2}W_0)}{g(i^{3/2}\beta W_0)} \right]^{1/2} \right\} \quad g = \frac{J_0(\alpha)}{J_2(\alpha)} \quad (C.3)$$

d. Derivation of Optimal Diameter Ratio in Asymmetrical Bifurcation

Analogous to impedance matching at the junctions of electrical transmission lines, global resistance is obtained as:

$$Res = Res_0 + \left[\frac{1}{Res_1} + \frac{1}{Res_2} \right]^{-1} \quad (D.1)$$

Where subscript 0 denotes the mother and 1 and 2 denote the daughter branches. The aggregate function is obtained by subjecting Res to constant volume constraint as:

$$\phi = Res + \lambda V, \quad V = \pi(l_0 R_0^2 + l_1 R_1^2 + l_2 R_2^2) \quad (D.2)$$

By the use of the method of Lagrange multipliers, and deriving (ϕ) with respect to (R_0), (R_1), and (R_2), three distinct equations would be achieved as (D.3) to (D.5), which should be solved.

$$\frac{\partial \phi}{\partial R_0} = 0 \rightarrow \lambda = \frac{i\omega\rho}{2\pi^2} \cdot \frac{1}{R_0^3} f(\alpha_0) \quad (D.3)$$

$$\frac{\partial \phi}{\partial R_1} = 0 \rightarrow \lambda = \frac{i\omega\rho}{2\pi^2} \cdot \frac{1}{R_1^3} f(\alpha_1) \cdot \frac{1}{\left[\left(\frac{Res_1}{Res_2} \right) + 1 \right]^2} \quad (D.4)$$

$$\frac{\partial \phi}{\partial R_2} = 0 \rightarrow \lambda = \frac{i\omega\rho}{2\pi^2} \cdot \frac{1}{R_2^3} f(\alpha_2) \cdot \frac{1}{\left[\left(\frac{Res_2}{Res_1} \right) + 1 \right]^2} \quad (D.5)$$

Considering (R) as branches diameter ratio ($R = R_2/R_1$), L as branches length ratio ($L = l_2/l_1$), and the defined equation for resistance to pulsatile flow in a tube, the ratio of resistance in daughters is simplified as follows:

$$\frac{Res_1}{Res_2} = \frac{R^2 g(\alpha_1)}{L g(\alpha_2)} \quad (D.6)$$

which can be shown in the form of (D.7)

$$\frac{\left(\frac{Res_1}{Res_2} \right) + 1}{\left(\frac{Res_2}{Res_1} \right) + 1} = \frac{R^2 g(\alpha_1)}{L g(\alpha_2)} \quad (D.7)$$

Combining (D.4), (D.5) and (D.7), yields the relation between (L) and (R) as the following:

$$L = R^{\frac{1}{2}} \frac{g(\alpha_1)}{g(\alpha_2)} \left[\frac{f(\alpha_2)}{f(\alpha_1)} \right]^{\frac{1}{2}} \quad (D.8)$$

The combination of (D.3), (D.4), (D.6), and (D.8), results in the relation between bifurcation branches radius as:

$$R_0^3 = \frac{f(\alpha_0)}{f(\alpha_1)} \left[R_2^3 \frac{f(\alpha_1)}{f(\alpha_2)} + 2(R_1 R_2)^{\frac{3}{2}} \left(\frac{f(\alpha_1)}{f(\alpha_2)} \right)^{\frac{1}{2}} + R_1^3 \right] \quad (D.9)$$

If the diameter ratio of the first and second daughter to the mother is defined as ($\beta = D_1/D_0$) and ($\gamma = D_2/D_0$), respectively, the (D.9) equation can be expressed as follows:

$$\frac{f(\alpha_0)}{f(\gamma\alpha_0)} \left[\beta^3 \frac{f(\gamma\alpha_0)}{f(\beta\alpha_0)} + \gamma^3 + 2(\beta\gamma)^{\frac{3}{2}} \left(\frac{f(\gamma\alpha_0)}{f(\beta\alpha_0)} \right)^{\frac{1}{2}} \right] = 1 \quad (D.10)$$

$$\alpha_0 = i^{3/2} W_0$$

e. Derivation of Optimal Asymmetrical Bifurcation Angles:

The overall procedure of obtaining optimal angles for asymmetrical bifurcations is the same as symmetric ones. The main difference is that (B.4) as the controlling equation would be substituted with the following:

$$\psi(R_0, \alpha_0) \delta l_0 + \psi(R_1, \alpha_1) \delta l_1 + \psi(R_2, \alpha_2) \delta l_2 = 0 \quad (E.1)$$

where the small displacement δ of the bifurcation point along the mother branch (E.2) and the first daughter branch (E.3) and the second daughter branch (E.4) should be substituted in (E.1).

$$\delta L_0 = \delta, \delta L_1 = -\delta \cos(\varphi_1), \delta L_2 = -\delta \cos(\varphi_2) \tag{E.2}$$

$$\delta L_0 = -\delta \cos(\varphi_1), \delta L_1 = \delta, \delta L_2 = \delta \cos(\varphi_1 + \varphi_2) \tag{E.3}$$

$$\delta L_0 = -\delta \cos(\varphi_2), \delta L_1 = \delta \cos(\varphi_1 + \varphi_2), \delta L_2 = \delta \tag{E.4}$$

Solving these equations simultaneously yields the following as the relation between bifurcation angles and branch radius:

$$\begin{aligned} \cos(\varphi_1) &= \operatorname{Re} \left\{ \frac{a_0^2 + a_1^2 - a_2^2}{2a_1a_0} \right\} \\ \cos(\varphi_2) &= \operatorname{Re} \left\{ \frac{a_0^2 + a_2^2 - a_1^2}{2a_2a_0} \right\} \\ \cos(\varphi_1 + \varphi_2) &= \operatorname{Re} \left\{ \frac{a_0^2 - (a_1^2 + a_2^2)}{2a_1a_2} \right\} \end{aligned} \tag{E.5}$$

where the coefficients in (E.5) are defined as the following relations:

$$\begin{aligned} a_1 &= C \left(i^{3/2} \cdot \gamma \cdot Wo \right) \cdot R_1 + R_1^2 \\ a_2 &= C \left(i^{3/2} \cdot \beta \cdot Wo \right) \cdot R_2 + R_2^2 \\ a_0 &= C \left(i^{3/2} \cdot Wo \right) \cdot R_0 + R_0^2 \end{aligned} \tag{E.6}$$

f. Derivation of Optimal Diameter Ratio in Symmetrical Bifurcation (Fourier Series Approximation)

For a periodic blood flow rate approximated by N complex Fourier modes as the following:

$$Q(t) = \sum_{n=0}^N Q_n e^{iwn t} \tag{F.1}$$

with forward pumping pressure gradient, and oscillating pressure gradients, resistance can be defined as:

$$\begin{aligned} Res &= \frac{8\mu}{\pi} \left(\frac{l_0}{R_0^4} + \frac{l_1}{2R_1^4} \right) + \\ &\frac{\omega\rho}{i\pi} \left[\frac{l_0}{R_0^2} \sum n \left(\frac{J_0(\alpha_{0n})}{J_2(\alpha_{0n})} \right) + \frac{l_1}{2R_1^2} \sum n \left(\frac{J_0(\alpha_{1n})}{J_2(\alpha_{1n})} \right) \right] \\ \alpha_n &= i^{3/2} \sqrt{n} Wo \end{aligned} \tag{F.2}$$

Substituting (F.2) in (A.4), and by the use of the method of Lagrange multipliers, and deriving (φ) with

respect to (R_0) and (R_1), the diameter ratio is obtained as:

$$\beta = \operatorname{Re} \left\{ \left[\frac{32 - i\beta^3 Wo^2 R_0 \sum_{n=1}^N n f(\beta\alpha_n)}{128 - i4Wo^2 R_0 \sum_{n=1}^N n f(\alpha_n)} \right]^{1/6} \right\} \tag{F.3}$$

g. Derivation of Optimal Symmetrical Bifurcation Angle (Fourier Series Approximation)

For a single unbranched vessel of length (l) with a periodic blood flow rate approximated by (N) complex Fourier modes, the (Res) might be defined as:

$$Res = \frac{8\mu l}{\pi r^4} + \sum \frac{ln\omega\rho}{i\pi r^2} \left[\frac{J_0(\alpha_n)}{J_2(\alpha_n)} \right] \tag{G.1}$$

Substituting (G.1) in (B.1) and differentiating with respect to radius (r), the cost function minimizes when:

$$Q^2 = \frac{\Gamma\pi^2}{\mu} \left[\frac{16}{r^6} - \frac{iWo^2}{2} \frac{1}{r^5} \sum n f(\alpha_n) \right]^{-1} \tag{G.2}$$

Substituting (G.2) in (B.1), the power dissipation per unit length is related to the radius of the vessel by:

$$\begin{aligned} \frac{W_{opt}}{l} &= \Gamma\pi\Upsilon \\ \Upsilon &= \left[\frac{16}{r^2} - \frac{iWo^2}{2} \frac{1}{r} \sum n f(\alpha_n) \right]^{-1} \left[8 - iWo^2 \sum n \frac{J_0(\alpha_n)}{J_2(\alpha_n)} \right] + r^2 \end{aligned} \tag{G.3}$$

Since there is an optimum bifurcation position where variation of overall cost due to small displacement is equal to zero, for a symmetrical bifurcation can conclude that:

$$\left[h(R_0, 1) + R_0^2 \right] \delta l_0 + 2 \left[h(R_1, \beta) + R_1^2 \right] \delta l_1 = 0 \tag{G.4}$$

Where $h(r, x)$ is defined as:

$$h(r, x) = \frac{8 - ix^2 Wo^2 \sum n \frac{J_0(x\alpha_n)}{J_2(x\alpha_n)}}{\frac{16}{r^2} - \frac{ix^2 Wo^2}{2r} \sum n f(x\alpha_n)} \tag{G.5}$$

Considering (B.5), (G.4) and (G.5), the optimum bifurcation angle (2θ) is obtained as:

$$\cos(\theta) = \frac{1}{2} \operatorname{Re} \left\{ \frac{h(R_0, 1) + R_0^2}{h(\beta R_0, \beta) + (\beta R_0)^2} \right\} \tag{G.6}$$